AD-A244 421

ENTATION PAGE

Form Approved
OMB No. 0704-0188

1. AGENCY USE ONLY	2. REPORT DATE	3. REPORT TYPE AND DATES COVERED
	10-9-91	Annual 6-1-90 - 6-30-91

(2)

4. TITLE AND SUBTITLE
Analog Processing of Optical Wavefront Using Integrated Guided-Wave Optics

5. FUNDING NUMBERS
F49620-90-C-0036

3151/00

6. AUTHOR(S)
Dr. Robert H. Rediker

7. PERFORMING ORGANIZATION NAME(S) AND ADDRESS(ES)
Research Laboratory of Electronics
Massachusetts Institute of Technology
77 Massachusetts Avenue
Cambridge, MA 02139

8. PERFORMING ORGANIZATION REPORT NUMBER

9. SPONSORING/MONITORING AGENCY NAME(S) AND ADDRESS(ES)
Air Force Office of Scientific Research
Building 410
Bolling Air Force Base, DC 20332

10. SPONSORING/MONITORING AGENCY REPORT NUMBER
3151/00

11. SUPPLEMENTARY NOTES
The view, opinions and/or findings contained in this report are those of the author(s) and should not be construed as an official Department of the Army position, policy, or decision, unless so designated by other documentation.

12a. DISTRIBUTION/AVAILABILITY STATEMENT
Approved for public release; distribution unlimited.

12b. DISTRIBUTION CODE

13. ABSTRACT *(Maximum 200 words)*

Work by Dr. Rediker and his collaborators is summarized here

92-01089

14. SUBJECT TERMS			15. NUMBER OF PAGES
			16. PRICE CODE
17. SECURITY CLASSIFICATION OF REPORT	18. SECURITY CLASSIFICATION OF THIS PAGE	19. SECURITY CLASSIFICATION OF ABSTRACT	20. LIMITATION OF ABSTRACT
UNCLASSIFIED	UNCLASSIFIED	UNCLASSIFIED	UL

NSN 7540-01-280-5500
Standard Form 298 (Rev. 2-89)
Prescribed by ANSI Std. 239-18
298-102

92 1 13 003

RESEARCH LABORATORY OF ELECTRONICS
MASSACHUSETTS INSTITUTE OF TECHNOLOGY
CAMBRIDGE, MASSACHUSETTS 02139

Analog Processing of Optical Wavefronts Using Integrated Guided-Wave Optics

Contract #F49620-90-C-0036

Annual Report
Period covered June 1, 1990 -- June 30, 1991

Submitted to the U.S. Air Force - Office of Scientific Research

Dr. Robert H. Rediker, Principal Investigator

September 30, 1991

Table of Contents

ANALOG PROCESSING OF OPTICAL WAVEFRONTS USING INTEGRATED GUIDED-WAVE OPTICS

Annual Report to the Air Force Office of Scientific Research
Contract #F49620-90-C-0036

June 1, 1990 – June 30, 1991

Robert H. Rediker
Massachusetts Institute of Technology
Department of Electrical Engineering and Computer Science
and Research Laboratory of Electronics

I. Introduction

Integrated Guided-Wave Optics has many advantages for the analog processing of optical wavefronts. These include small-size, high-speed, simplicity, reliability and reproducibility. The fabrication technique is similar to that of integrated circuits. The thrust of this program is to develop an integrated guided-wave optic system, in GaAs and GaAlAs for use at GaAs laser wavelength, to remove abberations from a laser beam and to steer the beam. The system would in addition have the capability to appropriately phase the outputs from a multiplicity of power amplifiers or injection-locked lasers. It is also the intent of the program to design and build the optical circuits so they are compatible with on-chip electronic circuits in order to minimize the required number of off-chip leads.

The research program has been proposed by MIT Research Laboratory of Electronics with part of the work being performed at MIT Lincoln Laboratory. In general, guided-wave component evaluation, analysis and understanding of optimization is performed at MIT Research Laboratory of Electronics, while the fabrication and actual optimization is performed at MIT Lincoln Laboratory.

It has been shown that integrated guided-wave optics can successfully be employed to measure and/or modify optical wavefronts.[1] The electrooptic material used was Ti:$LiNbO_3$. Recently, however, there have been significant advances in the use of semiconductors as the electrooptic material in which integrated optical devices are fabricated.[2] This program seeks to explore the fundamental issues associated with optical wavefront correction using integrated guided-wave devices in GaAlAs for use at GaAs/GaAlAs laser wavelengths.

In Section IIA the concept for correction of an optical wavefront is presented and several obvious advantages of "on-chip processing" are pointed out. Section IIB describes the operation of the proposed basic integrated-optics module for integrated guided-wave optics systems to do the required wavefront correction and steering. Many basic properties of guided-wave optics need to be better understood and optimized before the proposed concept can be realized in a practical manner.

The success of this program and many other integrated optics programs depends on the efficient collection of incident light and the efficient emission of laser light from the semiconductor. The fabrication, operation and optimization of reduced-confinement GaAlAs tapered waveguide antenna for use in coupling to free-space radiation was described[3,4], and described in detail in our final report for Air Force Contract #F49620-87-C-0043.

In the work described in this report we have focussed our attention on the requirements for optical phase difference measurement and correction, in addition to wavelength of operation, specific to the thrust of our program. In Section III we describe the design and development of an optical phase difference measurement technique that is independent of the power or power ratio in the interferometer arms. This technique has been incorporated into a proof-of-concept Mach Zehnder interferometer to demonstrate phase measurement and correction in a feedback system.

II. The Basic Module

A. Concept

The basic module proposed for wavefront correction is shown in Fig. 1. The system could contain as few as ten modules or as many modules as limited by reliability and reproducibility or other system considerations. Figure 1 is the same as Fig. 6 in the U.S. Patent[5] issued to the principal investigator, except it also includes the on-chip detector, voltage comparator and feedback control system. The advantages of this "on-chip processing" are the reduction of the number of leads that are required to come off the chip and the reduction of complexity of off-chip processing and time delays in signal transmission and processing. For example, in a system with 10^3 modules, only one control set-voltage is required (one lead). Without on-chip processing 10^3 voltages V_N need to be determined by the off-chip processor and require up to 10^3 leads to impress these voltages. It should be pointed out that there is a 2π radians (360°) ambiguity in the phase of the output from any waveguide. The voltage, V_N, need never exceed $V_{2\pi}$, the voltage across the waveguide electrodes to produce a change in the phase of 2π radians. Of course the incoming aberrated beam will be distorted by much more than 2π radians over the aperture of 10^3 modules. A second lead to the chip is required for on-chip $V_{2\pi}$ corrections to keep all V_N to correspond to phase shifts between 0 and 2π. For example if the aberration over the aperture is 50π and $V_{2\pi}$ = 20 V, then without the successive $V_{2\pi}$ corrections V_N would equal 500 V, which is not feasible for many fundamental and practical reasons.

While the module shown in Fig. 1 is specific to removing aberrations in the wavefront or steering the beam, using the same basic components other figures in the aforementioned patent illustrate the focussing of the wavefront. In general, analog processing of the optical wavefront is possible with various configurations of the components illustrated in Fig. 1.

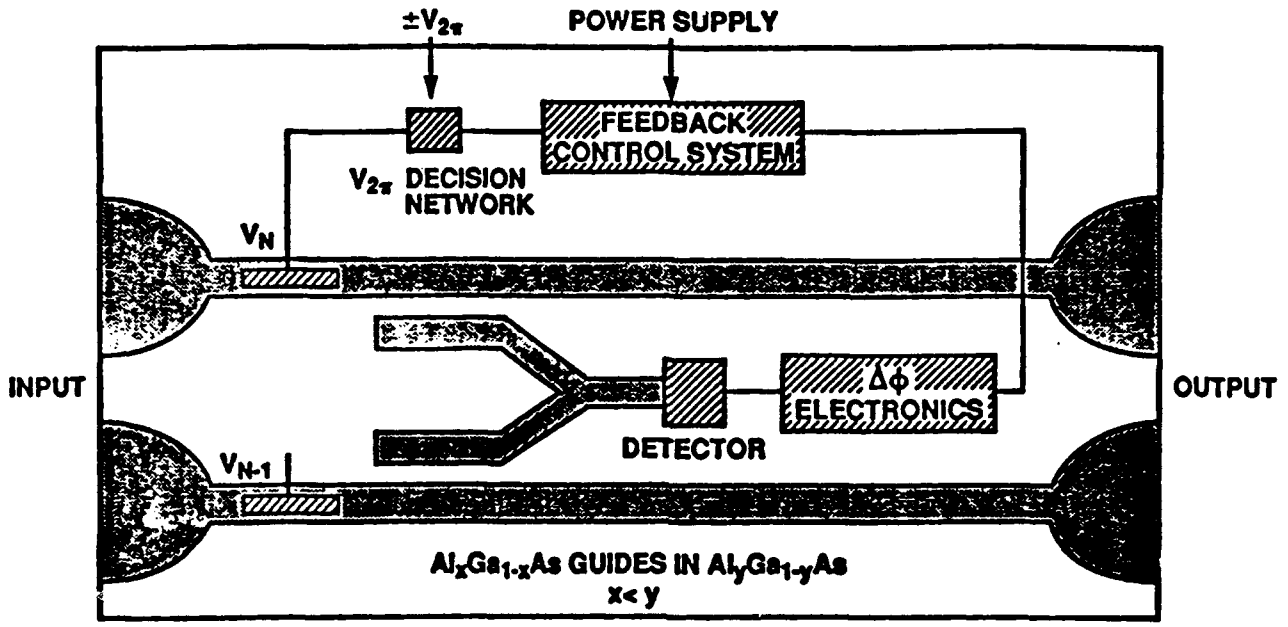

Fig. 1 The basic module for wavefront correction. In practice of the order of 10^3 modules may be appropriate for high-resolution correction. A significant advantage of the concept is the on-chip processing which reduces dramatically the number of leads required to come off the chip. The guides have a lower fraction, x, of Al in the $Al_xGa_{1-x}As$ than the fraction, y, in the substrate for dielectric confinement of the electromagnetic wave.

B. The Operation of the Basic Module

The operation of the basic module in Fig. 1 is as follows: The voltage V_N delays the phase of the optical wave in waveguide N by ϕ_N and the voltage V_{N-1} delays the phase of the optical wave in waveguide (N-1) by ϕ_{N-1} so that the two waves emerge from the waveguides in phase (the aberration is removed) or at a predetermined phase (the aberration is removed and the beam is steered). Evenescent wave coupling is used to couple a small fraction δ of the power in each straight-through waveguide to the adjacent arm of the interferometer between the waveguides. For equal incident optical powers, P, incident on each waveguide and equal evanescent coupling, δ, to each interferometer arm, the optical power incident on the detector is

$$P_{\Delta\phi} = [2\delta P \cos^2 \frac{\phi_N - \phi_{N-1}}{2}] B \qquad (1)$$

where B takes into account additional losses in interferometer arms such as due to the bends. When the powers P are unequal and/or the couplings δ, are unequal eq. (1) contains additional terms as is discussed in Section III below. Also presented in Section III are techniques to measure ($\Delta\phi = \phi_N - \phi_{N-1}$) independent of the powers P, the couplings δ and the losses taken into account by B. In integrated optics as in integrated circuits it is important for operation to be independent of individual component variations. For maximum output of the detector in Fig. 1 the feedback control system will set the value of V_N with respect to $V_{(N-1)}$ so that the phase shift ($\phi_N - \phi_{N-1}$) between the outputs of the two straight waveguides is zero. The details of the feedback control system are not described here, except to mention that it is a relatively straightforward system which nulls the detector output. As part of the electronic circuit, as mentioned earlier, there is a "$V_{2\pi}$ decision network" to reduce V_N below the maximum value of the voltage $V_{2\pi}$ which produces a phase shift of 2π radians (360°). Subtracting (or adding if V_N is

negative) $V_{2\pi}$ does not change the phase of the output from the straight-through waveguide.

III. Wavefront Phase Tilt Measurement

In the wavefront sensing and correction basic module, the input powers to the interferometer arms will not be equal, as a result of input power nonuniformity or unequal coupling by the evanescent couplers. The requirement that the coupling of the evanescent couplers be equal for a system with a large number of modules (10^3 - 10^4) is unrealistic. In integrated optics, as in integrated circuits, it is important to relax the requirements on individual components and require that the operation of the integrated optics (circuits) be independent of significant component variations. Therefore an optical wavefront phase tilt measurement technique has been developed to measure the wavefront phase tilt regardless of power non-uniformity.

The output power of a Y-junction interferometer with equal powers in the input arms is given by Equation 1. For unequal powers and unequal evanescent coupling from the straight-through waveguides to the interferometer arms, the output power of the Y-junction is given by,

$$P_{out} = [\delta_1 P_1 + \delta_2 P_2 + 2/\delta_1 P_1/\delta_2 P_2 \cos\phi] B \qquad (2)$$

where P_1 and P_2 are the unequal incident powers, δ_1 and δ_2 are the unequal coupling coefficients of the evanescent couplers, B again accounts for additional losses in the interferometer arms, and ϕ is the phase difference between the arms. Extracting the phase difference ϕ from this equation requires measuring the powers in the output arms, the coupling from each evanescent coupler, and the loss in the arms of the interferometer.

The Y-junction interferometer technique, shown in Fig. 2, used for the phase measurement is similar to dither techniques used in optical fiber sensors[5] and phase-locked interferometry.[7] If a sinusoidal phase dither $\Gamma \sin \omega t$ is applied

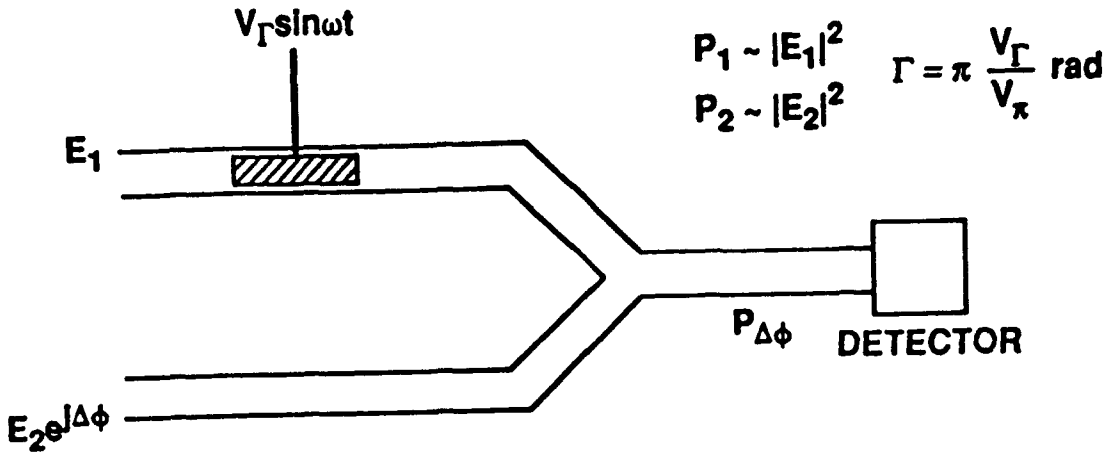

Figure 2. Y-junction optical phase difference measurement technique that is independent of the input power or power ratio of the interferometer arms.

to one arm of a Y-junction interferometer, the detected output power $P_{\Delta\phi}$ is given by

$$P_{\Delta\phi} = (P_1 + P_2)/2 + \sqrt{P_1 P_2}\cos(\Delta\phi - \Gamma\sin\omega t) \tag{3}$$

where P_1 and P_2 are the powers in the interferometer arms and $\Delta\phi$ is the phase difference between the arms. By using a Bessel function expansion for the cosine-sine term in Eq. (3), the following expressions for the amplitudes of the first $A(\omega)$ and second $A(2\omega)$ harmonics are obtained:

$$A(\omega) = 2\sqrt{P_1 P_2}J_1(\Gamma)\sin\Delta\phi \tag{4a}$$

$$A(2\omega) = 2\sqrt{P_1 P_2}J_2(\Gamma)\cos\Delta\phi \tag{4b}$$

where $J_1(\Gamma)$ and $J_2(\Gamma)$ are Bessel functions of the first kind of order 1 and 2 respectively. The phase difference between the arms can then be calculated using

$$\Delta\phi = \arctan\left[\frac{A(\omega)}{A(2\omega)}\frac{J_2(\Gamma)}{J_1(\Gamma)}\right] = \arctan\left[\frac{A(\omega)}{A(2\omega)}\frac{\frac{\Gamma^2}{8} - \frac{\Gamma^4}{96} + \cdots}{\frac{\Gamma}{2} - \frac{\Gamma^3}{16} + \cdots}\right] \tag{5}$$

where the number of significant terms required to evaluate the Bessel functions depends on the amplitude of the phase dither Γ. Note that the calculated phase difference is independent of the power or power ratio in the input arms of the interferometer.

This technique was incorporated into a proof-of-concept AlGaAs Mach-Zehnder interferometer, shown in Fig. 3, to demonstrate phase measurement and correction. The input power is divided between the interferometer arms. Phase modulators are used to apply a sinusoidal phase dither, to set a phase difference between the arms, and to correct the phase difference. A high voltage V_{abs} applied to the fourth modulator creates a power imbalance by absorbing power in one arm via electroabsorption, in addition to a phase change. $P_{\Delta\phi}$ is detected off chip, the

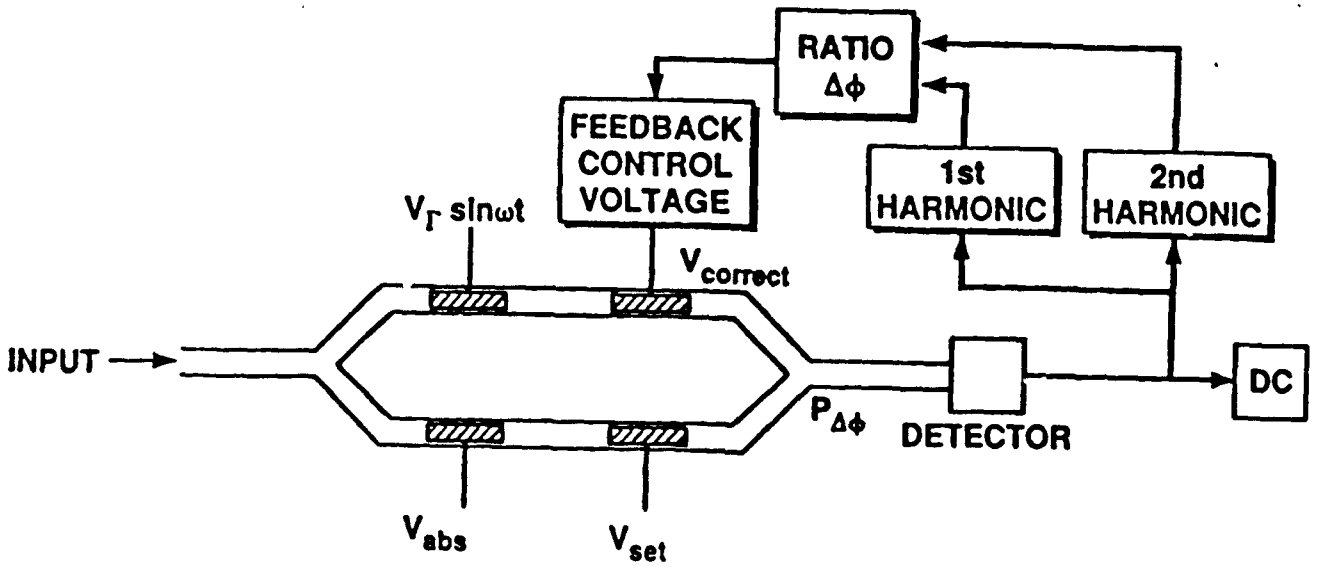

Figure 3. Proof-of-concept AlGaAs Mach-Zehnder interferometer system for demonstrating phase measurement and correction independent of power or power ratio in the interferometer arms.

amplitudes of the first and second harmonics are measured, $\Delta\phi$ is calculated from the ratio, and $V_{correct}$ is updated. The dc output of the interferometer, which is a maximum when $\Delta\phi = 0$, is also monitored. While the final goal is to monolithically integrate the optical and electronic components, this system utilizes off-chip circuitry and computer control of the feedback loop.

The interferometer was fabricated using a dielectric-loaded strip waveguide structure, illustrated in Fig. 4. The epilayers were grown by organometallic vapor phase epitaxy and the rib was etched in the upper cladding of the waveguide structure by chlorine reactive ion etching for two-dimensional optical confinement. This four-layer structure was modelled theoretically and single-mode waveguides designed to minimize absorption loss (low carrier concentration in the waveguide layer, scattering loss (the optical mode is away from the etched interfaces), and radiation loss in abrupt bends and Y-junctions (the optical mode is well-confined). The waveguide propagation loss was <1 dB/cm measured at 862 nm by a Fabry-Perot technique.[8] Measurements were made to characterize the angular dependence of the abrupt bend insertion loss and Y-junction insertion loss and are shown in Fig. 5. For the maximum angles used in the Mach-Zehnder interferometers, the abrupt bend insertion loss was ~0.20 dB/bend for a 0.5° angle and the Y-junction insertion loss was 0.37 dB for a 1.0° full angle.

Phase modulators were fabricated by a selective Be ion implantation, followed by rapid thermal annealing, to form a p^+-n-n^+ structure. The phase in the waveguides was modulated via the electrooptic effect by reverse biasing the p-n structure. The V_x voltage of these phase modulators was ~6.8 V for a 2 mm modulator. The composition of the epilayers was chosen to minimize electroabsorption at the desired operating wavelengths and voltages. These phase modulators were modelled both by a perturbation analysis and a more exact analysis of the waveguide in the presence of an electric field. Measurements by photoluminescence (to determine composition), stripping Hall (to determine p-n junction depth), and CV (to

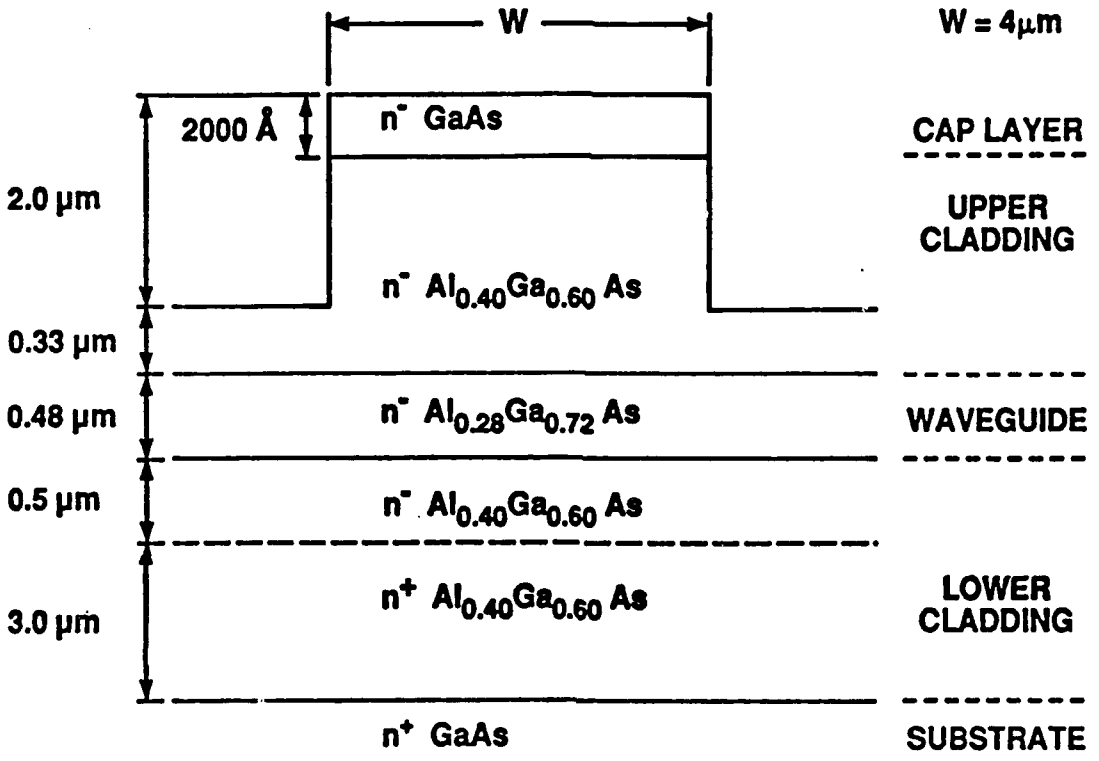

Figure 4. Cross section of the dielectric-loaded strip heterostructure waveguide for use at GaAs wavelengths. For the phase modulator sections, part of the upper cladding was doped p^+ (with the p^+-n junction located about 0.5 μm from the waveguide-cladding interface), and a AuZnAu top contact was used.

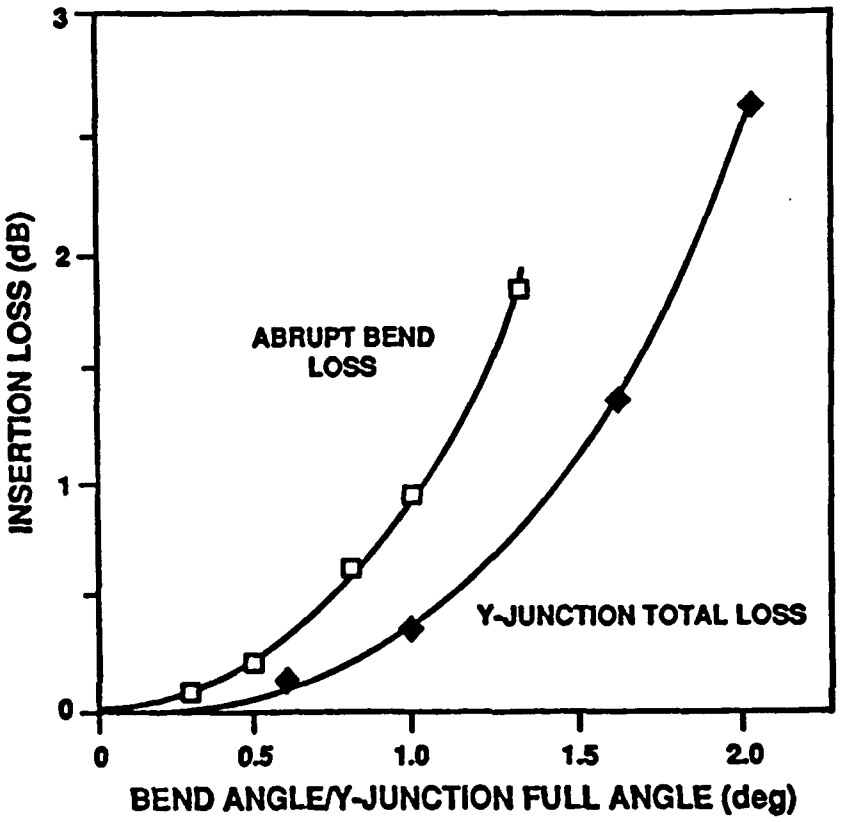

Figure 5. Measurements of the angular dependence of the abrupt bend insertion loss and Y-junction insertion loss.

determine carrier concentration profile) were used to model fabricated devices. A comparison of the theoretical analyses for phase modulation and experimental results for a 2 mm modulator are shown in Fig. 6.

The breakdown voltage of these phase modulators was ~47 V, so a maximum applied voltage of 42 V was chosen for these experiments. The correction voltage was limited to a range slightly larger than $V_\pi/2$ to $5V_\pi/2$, corresponding to a range in phase shift slightly larger than 2π. This was done to ensure that the modulator was always reverse biased and to minimize electroabsorption. The sinusoidal phase dither was applied to a 1 mm modulator (with $V_\pi \sim 12.4$ V). Typically, the dither signal had a peak voltage amplitude V_Γ of 1.0 V (amplitudes up to 5.0 V have been used) and a frequency of 500 Hz. The Bessel functions in Eq. (5) were calculated using the first two terms and the simple linear relationship for the amplitude of the phase dither $\Gamma = \pi V_\Gamma / V_\pi$. The experimental set-up used for testing the Mach-Zehnder interferometers is shown in Fig. 7. The output from a collimated laser is polarized TE and coupled into the input of the Mach-Zehnder interferometer by a 20x microscope objective. The Mach-Zehnder output can be directed using the switching mirror of a microscope to either a CCD camera for observation, or to a detector for power output measurements. Probe stations were usually used to apply voltages to the four phase modulators.

The AlGaAs Mach-Zehnder interferometer system was initially operated without feedback to characterize the phase measurement technique as a function of voltage-induced phase differences. A voltage V_{set} was applied to one arm to create a phase difference between the interferometer arms, and the amplitudes of the first and second harmonics were measured and used to calculate $\Delta\phi$. The interferometer dc output was also monitored. As V_{set} was increased above 25 V, a decrease in the peak amplitude of the dc output indicated that the power in one arm decreased because of electroabsorption. The phase difference between the interferometer

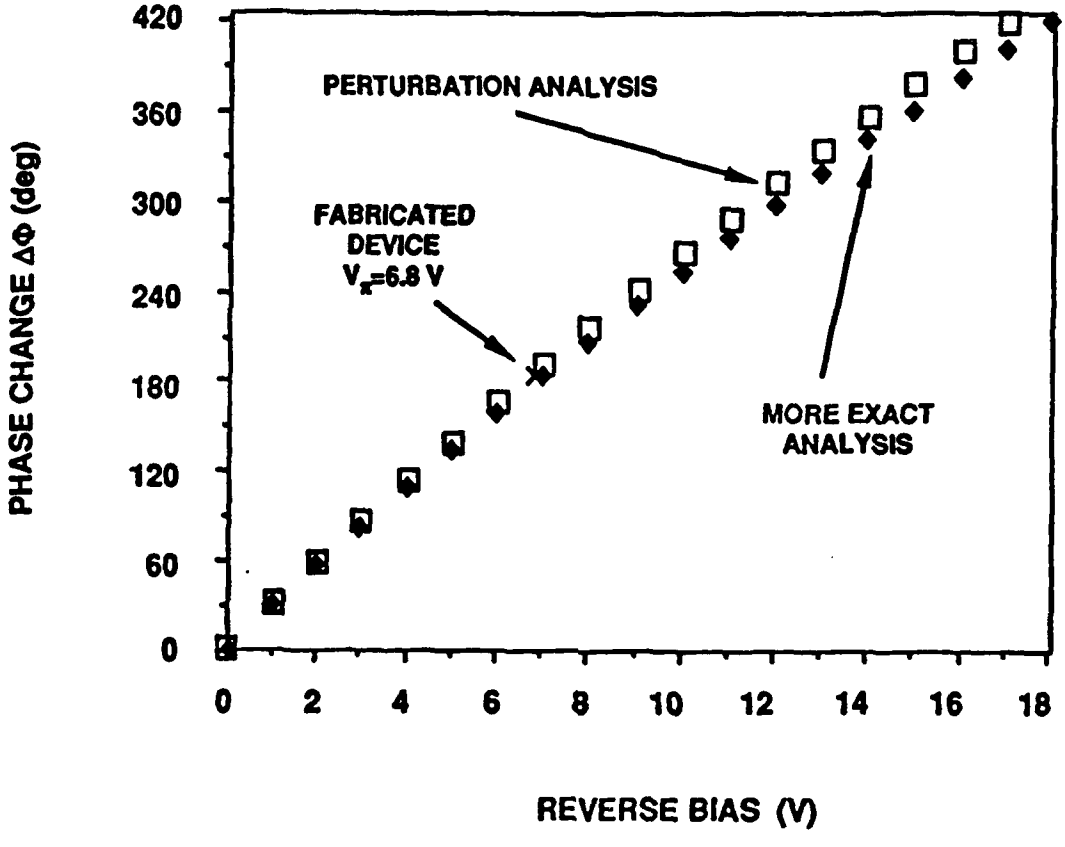

Figure 6. Comparison of the experimental results measured for a 2 mm long modulator with the modulation predicted by the perturbation and more exact analyses.

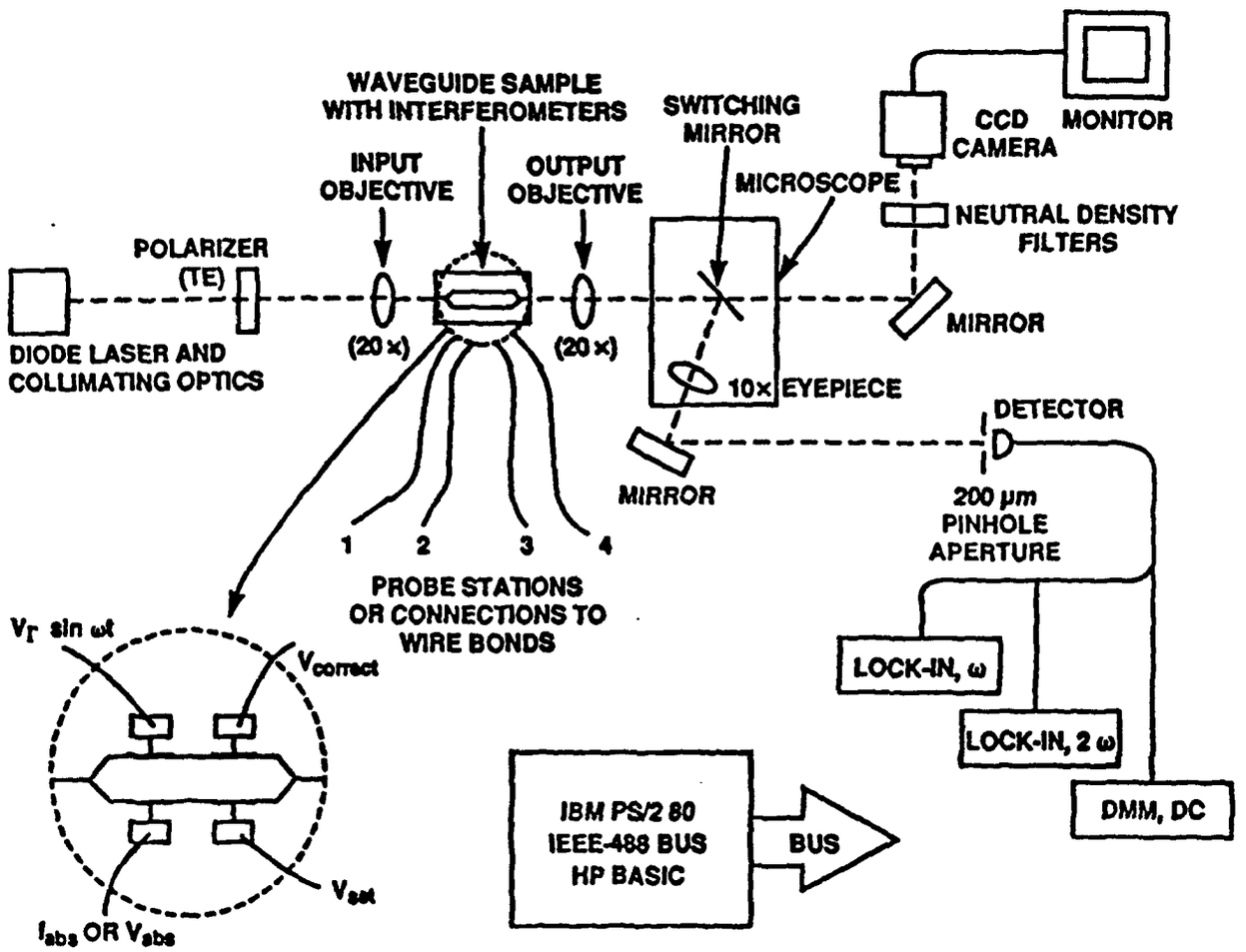

Figure 7. Experimental set-up for demonstrating optical phase difference measurement and correction using a proof-of-concept Mach-Zehnder interferometer.

arms was calculated between $-\pi/2$ and $3\pi/2$. The choice of phase range was arbitrary and could be any 2π range. The calculated $\Delta\phi$ increased linearly with V_{set} over each $-\pi/2$ to $3\pi/2$ range and was in agreement with the observed cosine-squared dependence of the dc output of the Mach-Zehnder interferometer.

With feedback, as shown in Fig. 3, a phase difference was again created by applying V_{set}, the first and second harmonics were measured, and $\Delta\phi$ was calculated. If $\Delta\phi \neq 0$, then $V_{correct}$ was updated, the harmonics were remeasured, and the new $\Delta\phi$ was calculated. This process was repeated until $\Delta\phi = 0$, that is, until the phase difference between the arms had been corrected. Then, a new V_{set} could be applied and the correction process repeated. The correction voltage was updated by assuming a simple linear relationship between phase and applied voltage. $\Delta\phi$ was divided by 2π and multiplied by the $V_{2\pi}$ voltage, and this result was added to the old correction voltage. The remainder of the update procedure consisted of limit checks (by adding or subtracting $V_{2\pi}$) to ensure that the correction voltage was within the specified range.

For the case shown in Fig. 8, V_{set} was increased in successive steps from 0 to 20 V. For each value of V_{set}, the first and second harmonics were measured and the phase calculated. Each step in V_{set} resulted in a corresponding increase in the phase difference, followed by phase-correcting cycles until $\Delta\phi = 0$ and phase correction had been attained. As expected, the dc output (not shown) decreased as each V_{set} increment was applied, and was maximized when the phase difference was corrected. Fig. 8(c) shows the updated $V_{correct}$ that was applied to correct the calculated $\Delta\phi$. Note that a $V_{2\pi}$ subtraction was required to keep $V_{correct}$ in the specified range. Phase correction was achieved to an accuracy of 0.0044 rad (or 0.25°). Correction was usually attained in 2 to 3 cycles for each step in an applied phase increment. Further improvements could be obtained with more sophisticated algorithms for the phase modulator characteristics (including any nonlinear effects). In this demonstration, the cycle time for

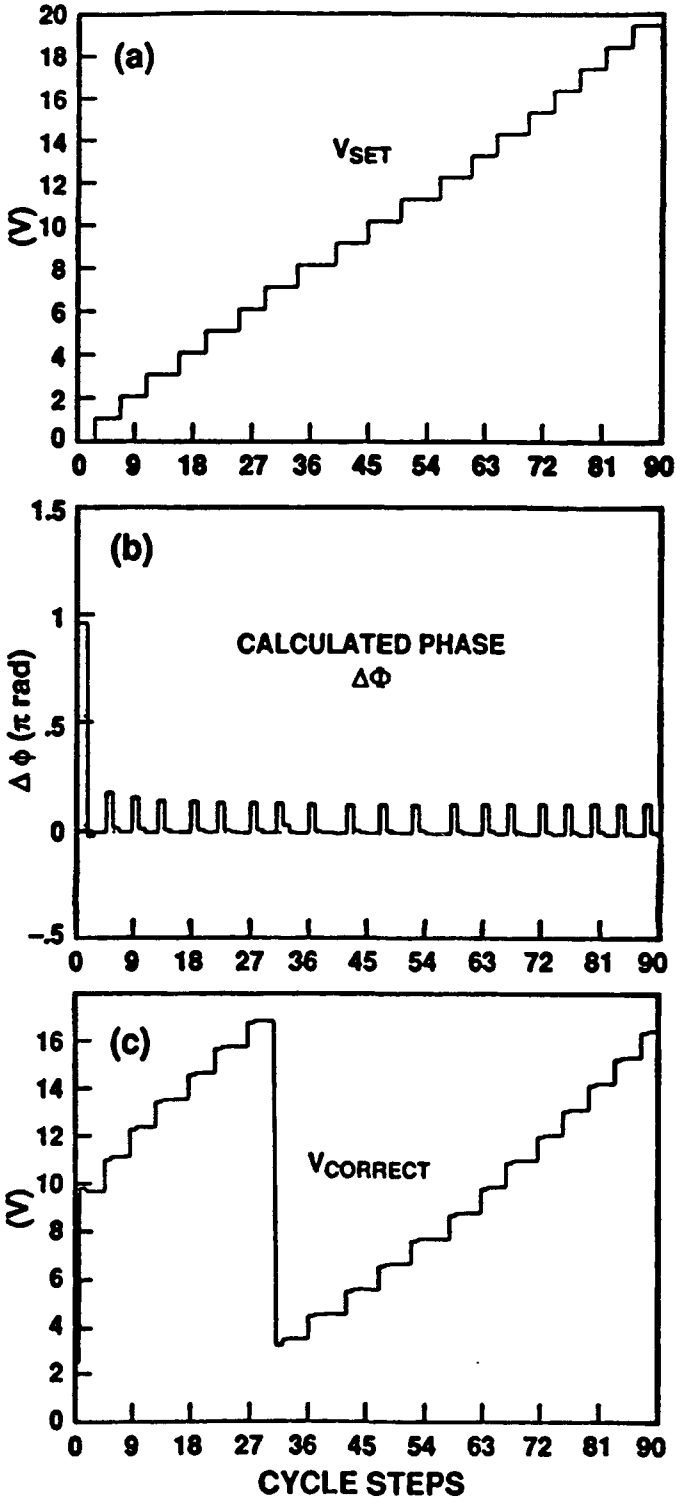

Figure 8. Results for the Mach-Zehnder interferometer system in the feedback mode: (a) V_{set} successively stepped from zero to 20 V, (b) the calculated phase difference $\Delta\phi$ between the interferometer arms, and (c) the applied correction voltage $V_{correct}$.

each phase-correcting cycle was a few seconds. This can be easily reduced to the order of milliseconds by increasing the dither frequency and using faster feedback electronics.

Results were also obtained for the case where a random number generator was used to generate random values for V_{set}, which resulted in random phase differences being applied between the interferometer arms. Phase correction again occurred in 2 to 3 cycles. Then, as a final test case, V_{set} was increased in successive steps from 20 to 40 V. In this range, in addition to phase change, there was increased electroabsorption in one arm of the interferometer so that a power imbalance was created between the arms. Phase measurement and correction proceeded as usual in 2 to 3 cycles with a 30% decrease in the power in one arm, which was observed by monitoring the dc output.

References

1. R.H. Rediker, T.A. Lind, and B.E. Burke, "Optical Wavefront Measurement and/or Modification Using Integrated Optics," J. Lightwave Tech., Vol. 6, pp. 916-932, 1988.
2. F.J. Leonberger and J.P. Donnelly, "Semiconductor Integrated Optic Devices," in Guided-Wave Optoelectronics, ed. T. Tamir (Berlin: Springer-Verlag, 1988).
3. D.E. Bossi, W.D. Goodhue, M.C. Finn, K. Rauschenbach, J.W. Bales, and R.H. Rediker, "Reduced-Confinement Antennas for GaAlAs Integrated Optical Waveguides," Appl. Phys. Lett., Vol. 56, pp. 420-422, 1990.
4. D.E. Bossi, W.D. Goodhue, L.M. Johnson, and R.H. Rediker, "Reduced-Confinement GaAlAs Tapered Waveguide Antennas for Enhanced Far-Field Beam Directionality," IEEE J. Quantum Electron., Vol. QE-27, no. 3, pp. 687-695, 1991.
5. R.H. Rediker, F.J. Leonberger, and D.P. Greenwood, "Method and Apparatus for Processing Optical Wave Signals," U.S. Patent 4,798,437, issued January 17, 1989.
6. T.G. Giallorenzi, J.A. Bucaro, A. Dandridge, G.H. Sigel, Jr., J.H. Cole, S.C. Rashleigh, and R.G. Priest, "Optical Fiber Sensor Technology," IEEE J. Quantum Electron., Vol. QE-18, no. 4, pp. 626-665, April 1982.
7. G.W. Johnson, D.C. Leiner, and D.T. Moore, "Phase-locked Interferometry," Opt. Eng., Vol. 18, no. 1, pp. 46-52, 1979.
8. M.W. Austin and P.C. Kemeny, "Measurement of Semiconductor Optical Waveguide Loss Using a Fabry-Perot Interference Technique," Integrated Optics, eds. H.-P. Nolting and R. Ulrich), Berlin: Springer-Verlag, pp. 140-143, 1985.